

# 3-D Investigation of Velocity Profile and Pressure Distribution in Bends with Different Diversion Angle

Rasoul Daneshfaraz\*

Department of Civil Engineering, University of Maragheh, Maragheh, Iran

\*daneshfaraz@maragheh.ac.ir

**Abstract-**This paper describes numerical investigation of velocity profile and pressure distribution of 3-D bends with different diversion angles via CFD model. Reynolds number, diversion angle and section angle, are introduced as important variable parameters of current study. Reynolds number's range was 100 to 1900 and the diversion angles of bends were 90, 135 and 180 degree with regard to inlet flow. The main goal of current study is to investigate the effect of Reynolds number and the diversion angle on velocity profiles and pressure distribution. It is worth mentioning that the experimental results of former study in a 90-degree bend are used for validating the numerical model. Studies of velocity profiles show that by increasing the section angle, the velocity profile inclines to outer wall, and maximum deviation from inlet velocity profile happens at 45 section angle. Also the maximum velocity occurs at 0.7 to 0.9 of the pipe diameter from inner wall. By increasing the section angle, the pressure profile inclines to outer wall and in this inclination, pressure loss is observed. For low Reynolds numbers, the variation of pressure loss is linear but by increasing the Reynolds number maximum pressure loss happens at limited section angle.

**Keywords-** Confined Flow; Bends; Reynolds Number; Velocity Profiles; Pressure Distribution

## I. INTRODUCTION

Flow in the bends is one of the primary characteristics of water conveying structures, related structure in dams and irrigation systems. Because of secondary circulation in the flow, the pattern of flow in the bends is complicated and these complications make it important issue in hydraulic engineering. The studies of current paper have been limited to pressure vessels and in this field, profile and contour of velocity in a 90 degree bend have been investigated by Bovendeerd et al. (1978) via finite element method. They used a laminar parabolic profile as the inflow condition. Also they provided a coherent description of the flow field throughout the bend, presenting the intensity of the secondary motions and the axial velocity profiles for different section along the bend. Bovendeerd et al. compared their results with former studies that used a uniform entry profile instead of a parabolic one and pointed out major differences in the flow development between the two conditions [1]. Van De Vosse (1989) modeled a three-dimensional 90 degree bend via finite element method and compared the numerical velocity profile with experimental results of Olsen (1971) [2] and observed the agreement [3]. The separated turbulent flow in U-shaped ducts (1999) is investigated by some researchers such as Chen and Hsieh [4]. Nakayama et al. (2003) performed their experimental studies on 180 degree duct and the result of measuring in separated zone and distribution of Reynolds stress are discussed by them. Separation in conical ducts under the effect of Reynolds number and divergence angle is investigated by Sparrow et al. (2009) and they presented some equations for ratio of dimensionless parameter of separation to diameter, versus Reynolds number and with regard to different divergence angle [6]. Sadeghfam and Akhtari (2012) simulated flow in the bend of closed sections with different diversion angle. They present some equations for length and thickness of separation zone with regard to their numerical studies [7].

In this study the pattern of flow in some bends with division angle of 90, 135 and 180 degrees with regard to inlet flow, has been investigated numerically and the effect of Reynolds number and division angle on velocity profile and pressure distribution has been assessed. It is worth mentioning that the flow mode is steady and the range of Reynolds number is 100 to 1900.

## II. GOVERNING EQUATION

The Navier–Stokes equations are nonlinear partial differential equations that describe fluids motion. In some cases, such as one-dimensional flow, the equations can be simplified to linear equations. The nonlinearity makes it difficult or even impossible for most of the problems to be solved. The nonlinearity is due to convective acceleration, which is an acceleration associated with the change in velocity over position. Hence, any convective flow, whether turbulent or not, will involve nonlinearity [8]. The general form of fluid motion is [9]:

$$\rho\left(\frac{\partial V}{\partial t} + V \cdot \nabla V\right) = -\nabla p + \nabla \cdot T + f \quad (1)$$

In Eq. (1),  $V$  is the flow velocity,  $\rho$  is the fluid density,  $p$  is the pressure, and  $f$  represents body forces (per unit volume) acting on the fluid.

Simplification of flow equation is done by two assumptions that are an incompressible flow and a Newtonian fluid.

Through this simplification the vector form of above equation is shown by Eq. (2). In this equation the shear stress term  $\nabla T$  becomes the useful quantity  $\mu\nabla^2V$ . It is worth mentioning that  $\mu$  is the (constant) dynamic viscosity [10].

$$\rho\left(\frac{\partial V}{\partial t} + V \cdot \nabla V\right) = -\nabla p + \mu\nabla^2V + f \quad (2)$$

The terms of Eq. (2) from left to right are, respectively, unsteady acceleration, convective acceleration, pressure gradient, viscosity and other body force [8]. For a steady flow in Cartesian coordinate system, above equation is simplified as Eqs. (3), (4) and (5) (the simulation of current study is done through these equations). The velocity components are typically named  $u$ ,  $v$ ,  $w$  and other parameters defined as above equations.

$$\rho\left(u\frac{\partial u}{\partial x} + v\frac{\partial u}{\partial y} + w\frac{\partial u}{\partial z}\right) = -\frac{\partial P}{\partial x} + \mu\left(u\frac{\partial^2 u}{\partial x^2} + v\frac{\partial^2 u}{\partial y^2} + w\frac{\partial^2 u}{\partial z^2}\right) \quad (3)$$

$$\rho\left(u\frac{\partial v}{\partial x} + v\frac{\partial v}{\partial y} + w\frac{\partial v}{\partial z}\right) = -\frac{\partial P}{\partial y} + \mu\left(u\frac{\partial^2 v}{\partial x^2} + v\frac{\partial^2 v}{\partial y^2} + w\frac{\partial^2 v}{\partial z^2}\right) + \rho g_y \quad (4)$$

$$\rho\left(u\frac{\partial w}{\partial x} + v\frac{\partial w}{\partial y} + w\frac{\partial w}{\partial z}\right) = -\frac{\partial P}{\partial z} + \mu\left(u\frac{\partial^2 w}{\partial x^2} + v\frac{\partial^2 w}{\partial y^2} + w\frac{\partial^2 w}{\partial z^2}\right) \quad (5)$$

Eqs. (6) and (7) are, respectively, the general and reduced form of continuity equation. Steady continuity equation for an incompressible flow and a Newtonian fluid is defined by Eq. (7).

$$\frac{\partial \rho}{\partial t} + \frac{\partial(\rho u)}{\partial x} + \frac{\partial(\rho v)}{\partial y} + \frac{\partial(\rho w)}{\partial z} = 0 \quad (6)$$

$$\frac{\partial u}{\partial x} + \frac{\partial v}{\partial y} + \frac{\partial w}{\partial z} = 0 \quad (7)$$

The components of velocity and pressure are obtained by solving Eqs. (3), (4), (5) and (7). In finite volume method, integration of Navier-Stokes equations is done over control volumes of solving domain. Various types of finite difference approximation are imposed to terms made in the integration equations of flow such as convection, diffusion and source terms. This operation turns integral equations to the system of algebraic equations. Then algebraic equations can be solved by repeating the procedure and calculating the residuals. This process will be continued to reach a minimum value for the residual and the model convergence.

### III. MODEL GEOMETRY, MESHING AND BOUNDARY CONDITION

In this study, the confined flow in bends is modeled three-dimensionally and the experimental results of Van De Vosse et al. are used for validating. The aforementioned bends have two arms that the degree of inclined arm with regard to inflow is 90, 135 and 180. The lengths of inlet and outlet arms are, respectively, 300 and 150 mm. It is worth mentioning that the value of curve radius for these bends is 24 mm.

Regarding small dimension and in order to eliminate the dimension effect, the results are discussed by dimensionless parameters. The 90-degree bend is illustrated in Fig. 1. In this figure  $a$  and  $R$  are, respectively, section radius and curve radius.

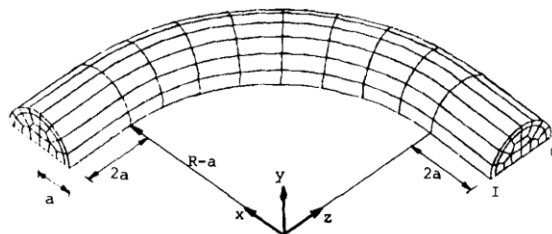


Fig. 1 The geometry of 90-degree bend

The variable parameters are Reynolds number (the investigated Reynolds numbers are 100, 300, 500, 700, 1000, 1300, 1600 and 1900), diversion angle (90, 135 and 180 degree with regard to inflow), and section angle on which velocity and pressure distribution are investigated (Table 1 shows the section angle for each bends). It is worth mentioning that the regime of flow is laminar and transition, also significant differences in results, are not observable with and without using turbulent models in transition range.

TABLE 1 SECTION ANGLES FOR EACH BENDS

| Bend Type         | Section Angle                                    |
|-------------------|--|
| <b>90-Degree</b>  | 0, 22.5, 45, 67.5 and 90                         |
| <b>135-Degree</b> | 0, 22.5, 45, 67.5, 90, 112.5 and 135             |
| <b>180-Degree</b> | 0, 22.5, 45, 67.5, 90, 112.5, 135, 167.5 and 180 |

Creating flow domain and meshing are done by Gambit preprocessor software. As an example, the geometry of 180-degree bend is illustrated in Fig. 2. In this figure the label A is used for inlet boundary and its type is velocity inlet. Boundary of wall is marked with B, and the C label is used for outlet of flow and its type is defined pressure outlet with regard to distribution of pressure.

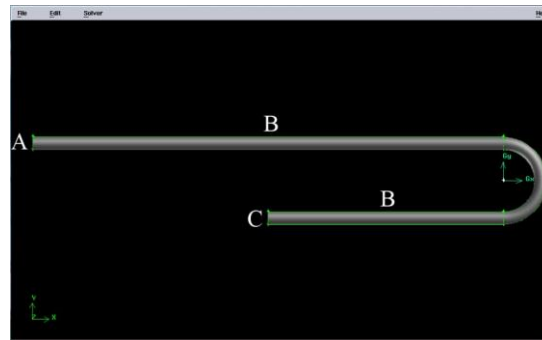


Fig. 2 The geometry of 180-degree bend and boundary condition

Regarding symmetry of geometry and in order to decrease numerical analysis, the boundary D is used as a symmetry boundary. This boundary is illustrated in Fig. 3 for 180-degree bend.

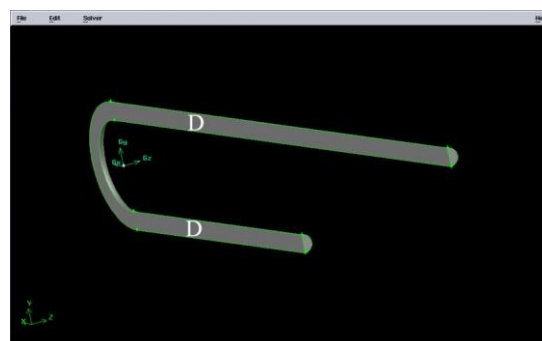


Fig. 3 180-degree bend and symmetry boundary

The type of meshing that is used in this study is map and hexagon and its number for 90, 135 and 180 degree bends are, respectively, 114114, 119196 and 124278. As a sample, meshing in 180-degree bend is illustrated in Fig. 4.

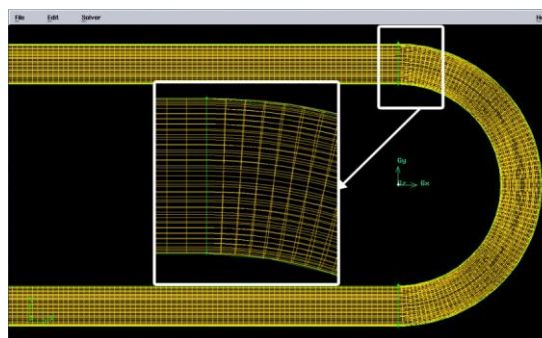


Fig. 4 180-degree bend and meshing

#### IV. NUMERICAL SOLUTION AND RESULTS

As mentioned before, numerical solution is done by Fluent, and Gambit preprocessor software is used for creating flow domain and meshing. In addition, standard scheme is used to discrete pressure. Quick scheme is used to separate momentum equations convection terms and also simple algorithm is used to couple the pressure and velocity. The coefficients smaller than 1 are applied for pressure, momentum and Reynolds stress to prevent from divergence.

The experimental results of Van De Vosse et al. and numerical result of this paper for a 90-degree bend are illustrated in Fig. 5. In this figure, good agreement between experimental results and the numerical results of current study is observable.

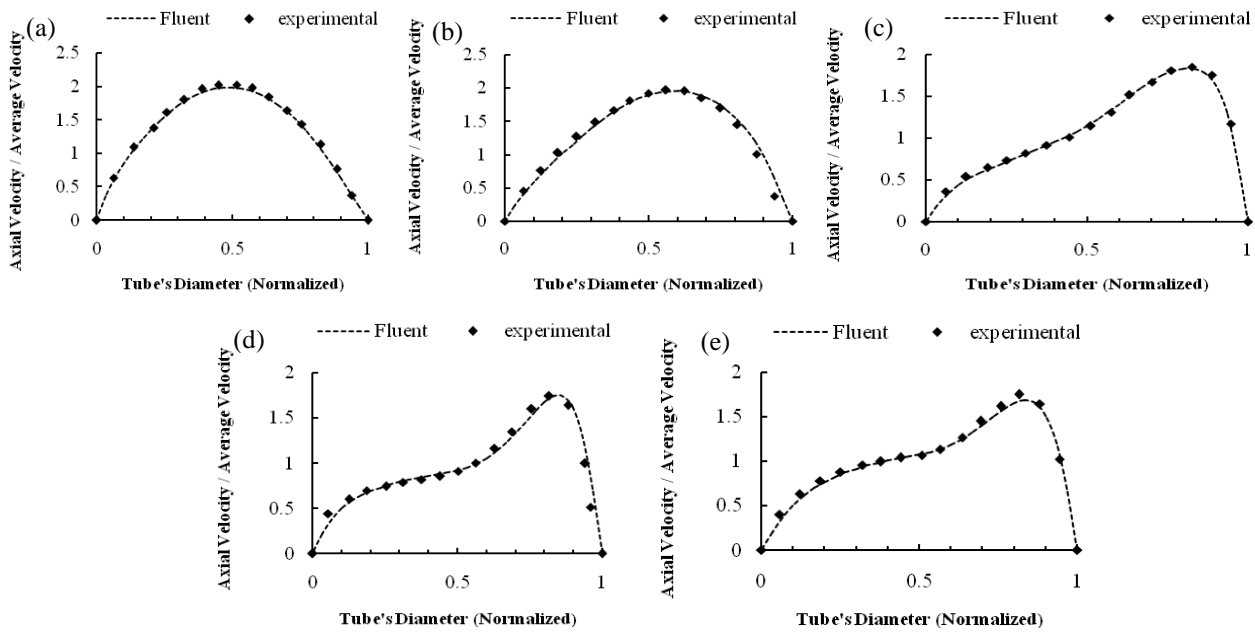


Fig. 5 Velocity profile for 90-degree bend and comparison between numerical and experimental results at different section angle. a) 0 degree, b) 22.5 degree, c) 45 degree, d) 67.5 degree, e) 90 degree

In this figure, both axes are dimensionless. The horizontal axis defined as tube's diameter (the values are normalized between 0 and 1) and the vertical axis shows the ratio of flow velocity to inlet average velocity.

Based on validated model, some bends with diversion angle of 90, 135 and 180 with degree regard to inlet flow in the range of Reynolds number between 100 and 1900, are analyzed numerically. The Figs. 6, 7 and 8, illustrate some samples of this investigation. According to these figures, velocity profiles incline to outer wall by increasing the section angle.

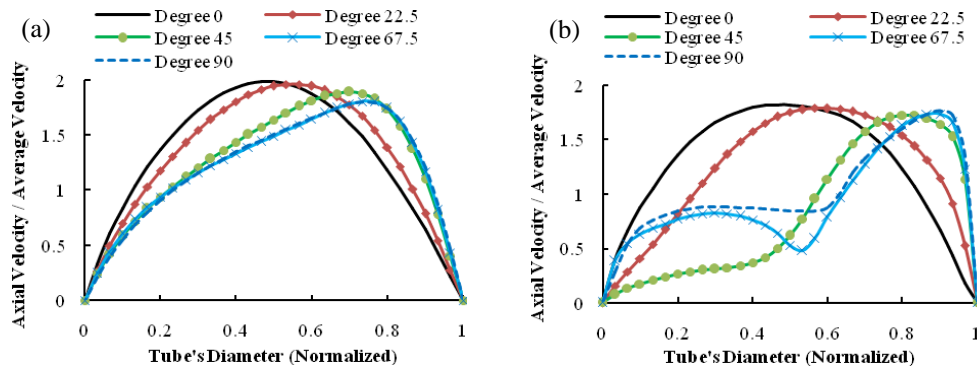


Fig. 6 Velocity profile for 90-degree bend at different section angle. a) Reynolds number of 100, b) Reynolds number of 1300

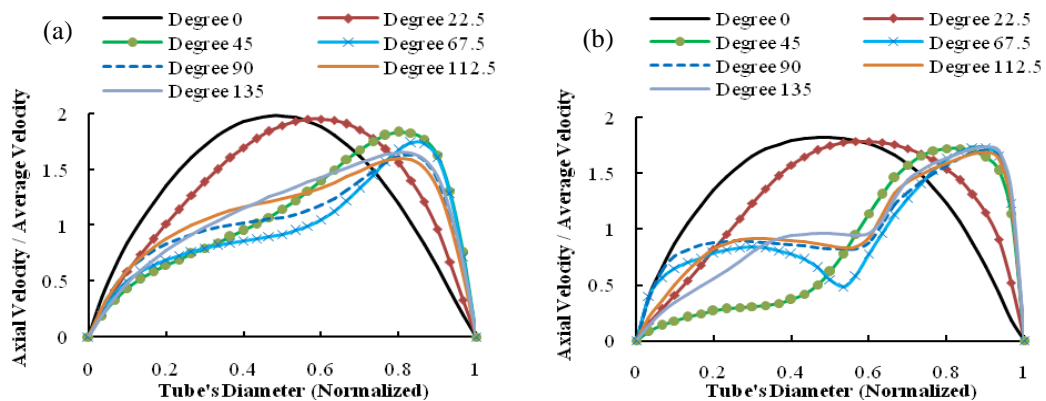


Fig. 7 Velocity profile for 135-degree bend at different section angle. a) Reynolds number of 300, b) Reynolds number of 1600

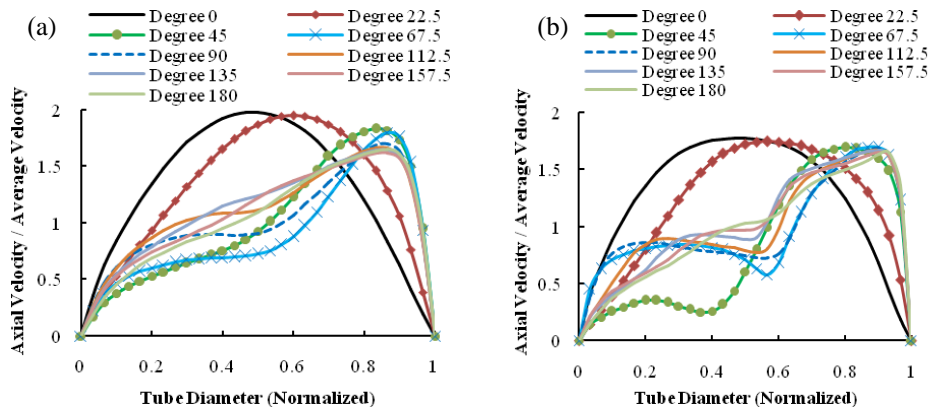


Fig. 8 Velocity profile for 180-degree bend at different section angle. a) Reynolds number of 500, b) Reynolds number of 1900

By comparing velocity profiles of mentioned bends, the same velocity profile is observed at equal section angle for different diversion angles. In other words and as an example, velocity profile at 45-degree section angle, is the same for 90, 135 and 180 diversion angle.

In order to investigate the velocity profile variations, deviation from velocity profiles is defined by deviation parameter (Eq. (8)).

$$D = \frac{\sum |V_{inlet} - V|}{n} \tag{8}$$

In Eq. (8),  $V_{inlet}$  is the inlet flow velocity,  $V$  is the velocity profile in bend,  $n$  is the number of velocity data, and  $D$  represents deviation parameter. The low values for  $D$  (close to 0) represent the least deviation from the velocity profiles. In Fig. 9, the variation of  $D$  versus section angle is illustrated. According to this figure by increasing the section angle, the  $D$  parameter first increases and then decreases. The maximum value for  $D$  is observed at section angle of 45 degree.

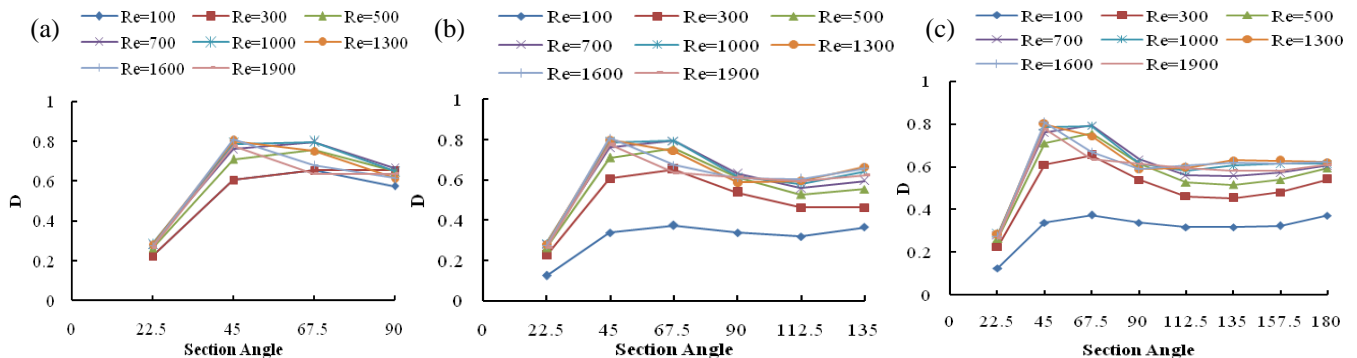


Fig. 9 Deviation from inlet velocity profile versus section angle. a) 90-degree bend, b) 135-degree bend, c) 180-degree bend.

Fig. 10 illustrates the location of maximum velocity (in outlet velocity profile) in 90, 135 and 180 degree bends. In this figure, the horizontal axis is defined as Reynolds number and the vertical axis represents tube's diameter. According to this figure, maximum velocity occurs at 0.7 to 0.9 of the pipe diameter from inner wall.

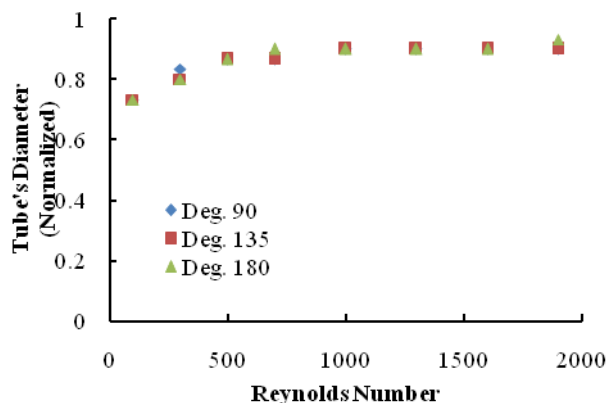


Fig. 10 The location of maximum velocity in outlet velocity profile

Based on numerical analysis in the Reynolds number range between 100 and 1900, pressure distributions were investigated at different section angles. In the following figures, both axes are dimensionless. The horizontal axis is defined as tube's diameter (the values are normalized between 0 and 1) and the vertical axis shows the ratio of flow pressure to inlet average pressure. According to these figures and similar to former section, pressure distribution inclines to outer wall by increasing section angle. The Figs. 11, 12 and 13 illustrate some samples of this investigation.

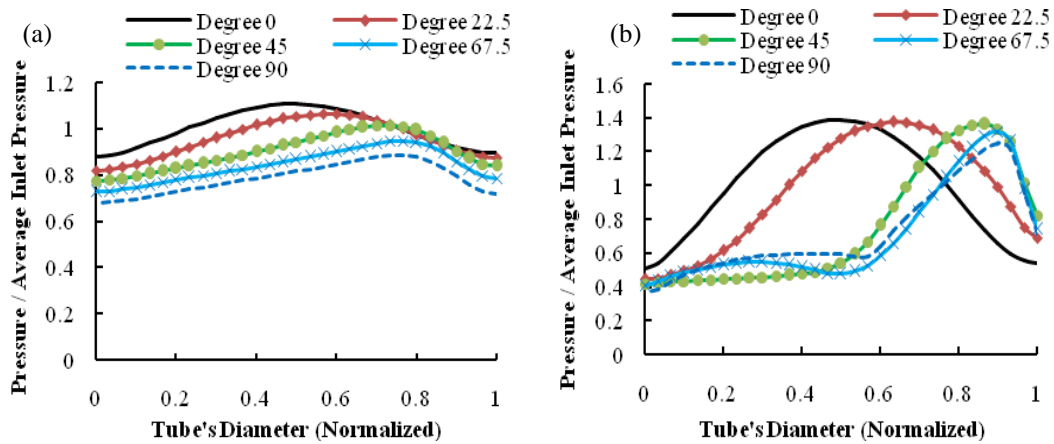


Fig. 11 Pressure distribution for 90-degree bend at different section angle. a) Reynolds number of 100, b) Reynolds number of 1300

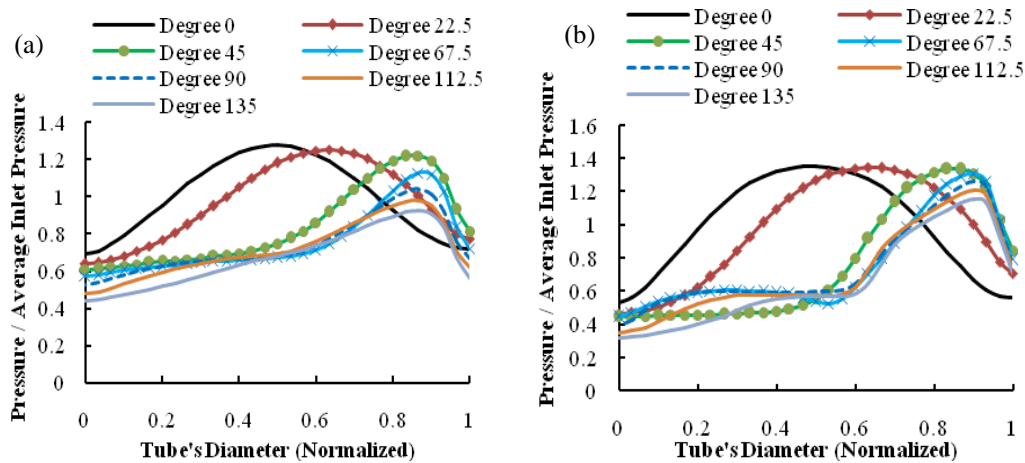


Fig. 12 Pressure distribution for 135-degree bend at different section angle. a) Reynolds number of 300, b) Reynolds number of 1600

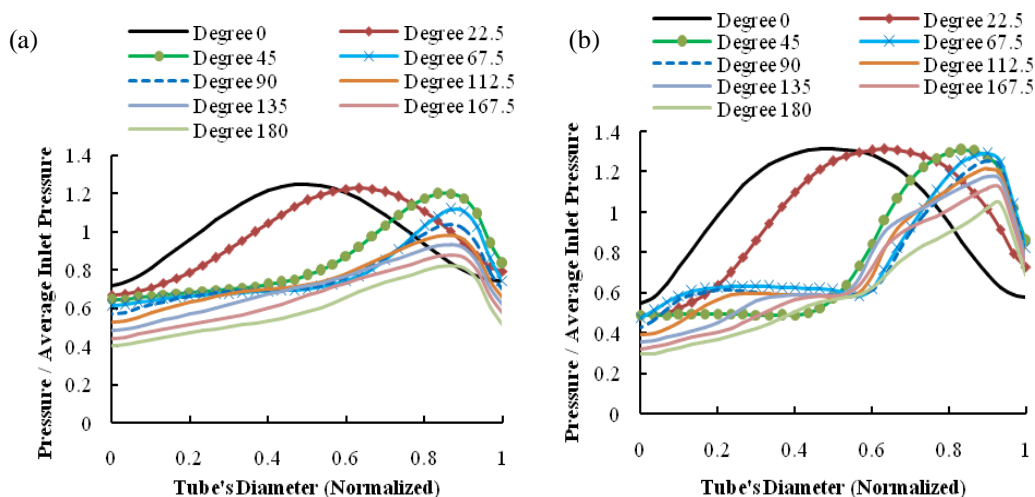


Fig. 13 Pressure distribution for 180-degree bend at different section angle. a) Reynolds number of 500, b) Reynolds number of 1900

By investigating the results of pressure distribution at different sections, the variations of pressure are illustrated in Fig. 14. In this figure, the horizontal axis is defined as section angle and the vertical axis shows the ratio of flow pressure to inlet average pressure. According to this figure, for low Reynolds numbers, the variation of pressure loss is linear and equal but by increasing the Reynolds number maximum pressure loss happens at section angle between 22.5 and 45 degree.

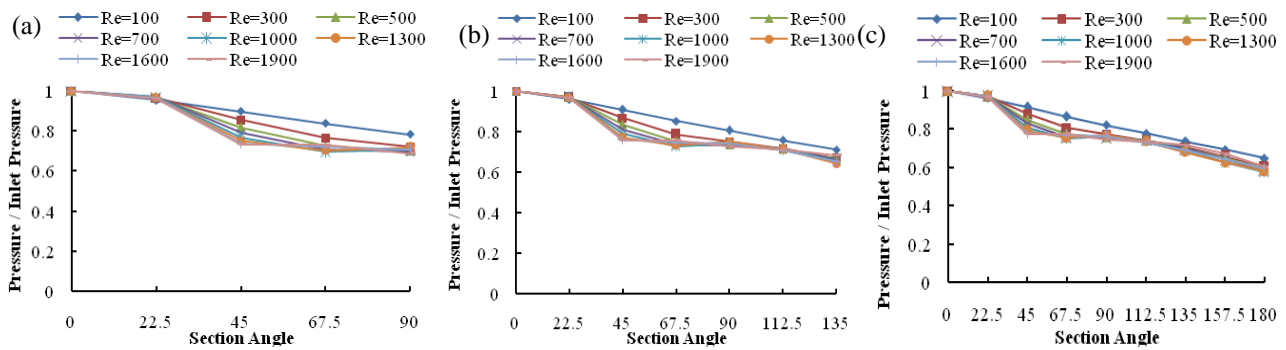


Fig. 14 Dimensionless parameter of pressure versus section angle. a) 90-degree bend, b) 135-degree bend, c) 180-degree bend

## V. CONCLUSION

In this study, the flow in some bends with different diversion angles (90, 135 and 180 degree regard to inflow direction) is simulated 3-dimensionally by CFD methods and the results are discussed. The experimental results of Van De Vosse et al. are used for validating the numerical model. It is worth mentioning that numerical analysis is done for steady flow in the Reynolds number range between 100 and 1900, and the results are presented at different section angles. By increasing the section angle, velocity profiles inclined to outer wall. The maximum deviation from inlet velocity profile was observed at section angle of 45 degree and maximum velocity occurs at 0.7 to 0.9 of the pipe diameter from inner wall. Likewise the same velocity profile at equal section angle for different diversion angle, is observed. Also by increasing the section angle, pressure distribution inclined to outer wall and in this inclination, pressure loss is observed. For low Reynolds numbers, pressure loss variations are linear and equal but by increasing the Reynolds number, the maximum pressure loss happens at section angle between 22.5 and 45 degree.

## REFERENCES

- [1] P. H. M. Bovendeerd, A. A. V. Steenhoven, F. N. V. D. Vosse, and G. Vossers, "Steady entry flow in a curved pipe," *Journal of Fluid Mechanics*, vol. 177, pp. 233-246, 1987.
- [2] Olson D. E. 1971. "Fluid mechanics relevant to respiration: flow within curved or elliptical tubes and bifurcating systems," Ph.D. Thesis, University of London, 1971.
- [3] F. N. Van De Vosse, A. A., Van Steenhoven, A. Segal, and J. D. Janssen, "A Finite element analysis of steady laminar entrance flow in a 90 Curved tube," *International Journal of Numerical Methods in Fluids*, vol. 9, pp. 275-287, 1989.
- [4] S.S. Hsieh, P.J. Chen, and H.J. Chin, "Turbulent flow in a rotating two pass smooth channel," *Journal of Fluids Engineering*, vol. 121, pp. 725-734, 1999.
- [5] H. Nakayama, M. Hirota, H. Fujita, T. Yamada, and Y. Koide, "Flow characteristics in rectangular ducts with a sharp 180-degree turn," *Transactions of the Japan Society of Mechanical Engineers*, vol. 69(681), pp. 1171-1179, 2003.
- [6] E.M. Sparrow, J.P. Abraham, and W.J. Minkowycz, "Flow separation in a diverging conical duct: Effect of Reynolds number and divergence angle," *Journal of Heat and Mass Transfer*, vol. 52, pp. 3079-3083, 2009.
- [7] S. Sadeghfam, and A. A. Akhtari, "Numerical investigation of length and thickness of separation zone after sudden change of direction in closed sections," *Journal of Civil Engineering and Urbanism*, vol. 2(1), pp. 35-39, 2012.
- [8] C. B. Parker, *McGraw Hill Encyclopedia of Physics*, 2nd ed. New York: McGraw Hill, 1994.
- [9] G. K. Batchelor, *An Introduction to Fluid Dynamics*, London: Cambridge University Press, 1967.
- [10] D. J. Acheson, *Elementary Fluid Dynamics, Oxford Applied Mathematics and Computing Science Series*. New York: Oxford University Press, 1990.